Zeros, dips, and signs in pp and $p\bar{p}$ elastic amplitudes

Flávio Pereira*
Observatório Nacional, CNPq, Rio de Janeiro 20921-400, Rio de Janeiro, Brazil

Erasmo Ferreira†
Instituto de Física, Universidade Federal do Rio de Janeiro, C.P. 68528, Rio de Janeiro 21945-970, Rio de Janeiro, Brazil

(Received 15 July 1999; revised manuscript received 5 November 1999; published 9 March 2000)

The dips observed in the differential cross sections of elastic pp and $p\bar{p}$ scattering are studied in terms of the locations of the zeros of the real and imaginary parts of the amplitude and of the sign of real part at large $|t|$. It is confirmed that the differences in shapes of the dips in the pp and $p\bar{p}$ systems are determined by a change of sign of the real tail, which seems to be determined by perturbative QCD contributions.

PACS number(s): 13.85.Dz, 12.38.Lg, 13.85.Lg

I. INTRODUCTION

In a previous work [1], a description of the high energy pp scattering was made using a parametrization inspired in the model of the stochastic vacuum (MSV) [2] to obtain the scattering amplitude directly from the data. The existence of a zero in the imaginary part of the amplitude is a common feature of both the MSV calculation and data, and the measured differential cross section requires that this zero be filled by the contribution of the real part. The profile functions obtained by a parametrization based on the MSV original form that describe in all details the experimental data serve as a reference pattern to help studies in hadron-hadron scattering. In the present work we improve the parametrization [1] in order to describe accurately the shapes of the dips and the zeros of the real and imaginary amplitudes, using the smoothness of the parametric representation as a strong constraint.

In a somewhat detailed dynamical scheme, Donnachie and Landshoff [3] described the structure of the dip in high energy scattering through the interference of single-Pomeron, double-Pomeron, and three-gluon exchanges, predicting that the dip in $p\bar{p}$ would be less pronounced than in pp scattering, and our present work exhibits the same structure, namely, that the differences between pp and $p\bar{p}$ scattering are represented by the change of sign of a term in the real part of the amplitude. We give particular attention to the locations of the amplitude zeros, showing the connection between the proximity of real and imaginary zeros and the depths of the dips.

We use the data on total cross section, slope parameter B and ratio $\bar{\rho}$ of the forward real to imaginary parts of the amplitudes in pp and $p\bar{p}$ scattering shown in Table I of our previous work [1], adding these quantities at 19.4 GeV, namely, $B=11.74\pm0.04$ GeV^{-2}, $\sigma^T=38.97\pm0.06$ mb, and $\bar{\rho}=0.019\pm0.016$, together with the differential cross section at the same energy [4(a)]. Most $d\sigma^{el}/dt$ measurements [4,5] are limited to $|t|<10$ GeV^2, while large angle data are available only at $\sqrt{s}=27.4$ GeV [6], presenting a $|t|$ dependence approximately of the form $|t|^{-8}$ [7], the magnitude of $d\sigma^{el}/dt$ at a given large $|t|$ being nearly energy independent [8]. The differential cross section at $\sqrt{s}=19.4$ GeV [6] for values of $|t|$ in the range 5–12 GeV^2 approach that of $\sqrt{s}=27.4$ GeV. In order to maintain the universality of the tail we have adopted in our parametrization for all energies between 19 and 63 GeV the same 27.4 GeV values for large $|t|$. In Sec. II the behavior of the dips of the differential cross section are described in terms of the locations of the zeros of the real and imaginary amplitudes, and the large $|t|$ behavior of the differential cross section of pp and $p\bar{p}$ systems is discussed.

The imaginary and real parts of the amplitude are respectively parametrized [1] in the forms

$$\mathcal{I}(t)\equiv\alpha_1 e^{-\beta_1|t|}+\alpha_2 e^{-\beta_2|t|}+\lambda 2\rho e^{\rho\gamma}A_\gamma(t) \tag{1}$$

and

$$\mathcal{R}(t)\equiv\alpha_1' e^{-\beta_1'|t|}+\lambda' 2\rho e^{\rho\gamma'}A_{\gamma'}(t), \tag{2}$$

where

$$A_\gamma(t)\equiv\frac{e^{-\gamma\sqrt{\rho^2+a^2|t|}}}{\sqrt{\rho^2+a^2|t|}}-e^{\rho\gamma}\frac{e^{-\gamma\sqrt{4\rho^2+a^2|t|}}}{\sqrt{4\rho^2+a^2|t|}}, \tag{3}$$

with $\rho=3\pi/8$, and we have grouped the factors $2\rho e^{\rho\gamma}A_\gamma(t)$ in order to have $2\rho e^{\rho\gamma}A_\gamma(0)=1$.

The dimensionless scattering amplitude and the elastic differential cross section are given, respectively, by

$$T(s,t)=4\sqrt{\pi}s[i\mathcal{I}(t)+\mathcal{R}(t)] \tag{4}$$

and

$$\frac{d\sigma^{el}}{dt}=\frac{1}{16\pi s^2}|T(s,t)|^2. \tag{5}$$

The simple exponential term $\alpha_1'\exp(-\beta_1'|t|)$ was included in the real part specifically to describe the large $|t|$(5

*Email address: flavio@on.br
†Email address: erasmo@if.ufrj.br

TABLE I. Values of parameters for Eqs. (3) and (4). $\alpha_1,\beta_1,\alpha_2,\beta_2,\lambda$, and λ' are in GeV^{-2}, and γ,γ' are dimensionless. $\alpha_1'=0.0031\ \mathrm{GeV}^{-2}$ and $\beta_1'=0.41\ \mathrm{GeV}^{-2}$ are the same for all ISR energies and 19.4 GeV.

$\sqrt{s}$	α_1	β_1	α_2	β_2	λ	λ'	γ	γ'	χ^2
19.4	1.7400	1.3398	2.8771	2.2098	9.4000	0.2632	3.7019	3.67	3.53
23.5	1.7298	1.4390	3.1091	2.2949	9.1850	0.2774	3.8625	5.00	1.18
30.7	1.8224	1.4502	3.1649	2.3299	9.5467	0.6073	3.9015	6.70	1.33
44.7	1.6699	1.5025	3.0000	2.1086	10.3650	0.9354	4.0306	6.65	4.36
52.8	1.8500	1.5287	2.9600	2.1753	10.4630	1.1913	4.0529	6.80	3.29
62.5	1.9272	1.5529	2.8081	2.1337	10.8201	1.4747	4.0921	7.35	1.76
546	2.6174	2.1539	3.9061	2.1813	15.7463	3.0270	4.8190	7.97	1.23
1800	3.1036	2.4526	4.4246	2.4253	18.3315	3.6204	5.3450	8.60	2.00

$<|t|<15\ \mathrm{GeV}^2$) data [6] at 27.4 GeV. This term is considered as universal for all pp and $p\bar{p}$ data, and a change of its sign leads from pp to the $p\bar{p}$ system. The exponential is numerically equivalent to $|t|^{-8}$ in the $|t|$ range of interest, and was used to avoid the singularity at the origin. This tail is not used in the description of the 546 and 1800 GeV data, where large $|t|$ values have not been measured.

The new values of the parameters are given in Table I, which is an update of our previous determination [1], and now includes the $\sqrt{s}=19.4$ GeV data. The smoothness of the energy dependence of all parameters must be remarked. In comparison to the previous values, the parameters γ and γ' have been slightly modified to improve the description of the data in the dip region of the pp differential cross sections as shown in Fig. 1 for $\alpha_1'>0$ (solid lines). The case

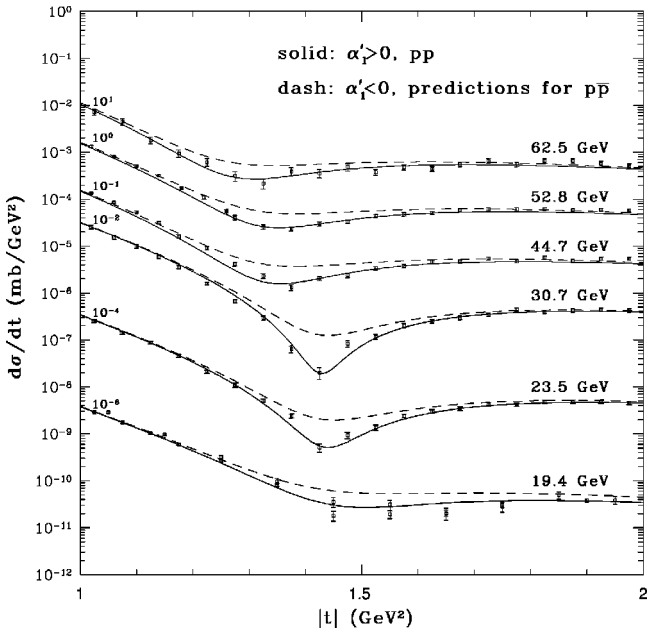

FIG. 1. Fittings of elastic differential cross sections through Eqs. (1) and (2) at 19.4 GeV and ISR energies, shown in an extended scale only in the region of the dips of pp scattering with $\alpha_1'>0$ (solid lines) and the predictions for $p\bar{p}$ scattering with $\alpha_1'<0$ (dashed lines). Curves and data at different energies are conveniently separated through multiplication by powers of 10.

$\alpha_1'<0$ (dashed lines), which applies to $p\bar{p}$ scattering, is discussed later.

II. ZEROS AND SIGNS OF THE AMPLITUDES

The characteristic shape of the dip region of the differential cross sections has been described by Donnachie and Landshoff [3] in terms of various mechanisms of Pomeron and gluon exchanges. The low $|t|$ region is described by the single-Pomeron exchange (P), which is dominant in this region and gives the value to the slope B. In order to describe the data, the double-Pomeron exchange (PP) was introduced with the magnitude of its imaginary part chosen so as to cancel that of the P mechanism in the region where a dip is to be formed. In addition to these contributions there is the gg (ρ,ω,f,A_2) exchange which also is important only at small $|t|$. To yield a dip, the real part of the P term is partially cancelled by the three-gluon exchange (ggg), which is dominant for large $|t|$, has opposite signs for pp and $p\bar{p}$ systems, and led to the prediction that at high energies the dips would be less pronounced in $p\bar{p}$ scattering . The other terms contributing at large $|t|$ are the two-gluon-one-Pomeron exchange (ggP) and the three pomeron exchange (PPP), but they have very little effect, the dominant term at large $|t|$ being $A_{ggg}(s,t)$. This term has the form [7]

$$A_{ggg}(s,t)=-\frac{N}{|t|}\frac{5}{54}\left[4\pi\alpha_s(|\hat{t}|)\frac{1}{m^2(|\hat{t}|)+|\hat{t}|}\right]^3, \qquad (6)$$

where $m^2(|\hat{t}|)$ is an effective gluon mass, $\alpha_s(|\hat{t}|)$ is the running coupling constant, $\hat{t}\simeq t/9$, $\Lambda=200$ MeV, and $m_0=340$ MeV, which for $\hat{t}\gg 1$ yields the $|t|^{-8}$ dependence of the large $|t|$ differential cross section. The normalization factor N is negative and determined by the proton wave function. We remark that our parametrization incorporates all information about the dynamical mechanisms of pp scattering and corresponds to the sum of all terms discussed by Donnachie and Landshoff.

According to phenomenological descriptions, the structure of forward pp scattering is determined mainly by the imaginary part of the amplitude which decreases exponentially from $|t|=0$ and vanishes with a zero located in the

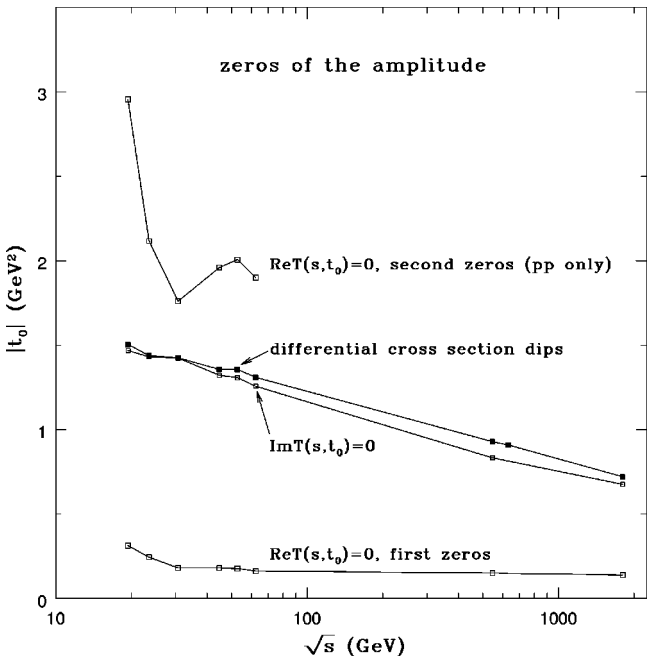

FIG. 2. Locations of the zeros of the imaginary and real parts of the scattering amplitude (white squares) and the positions of the dips of $d\sigma^{el}/dt$ (black squares) as functions of energy.

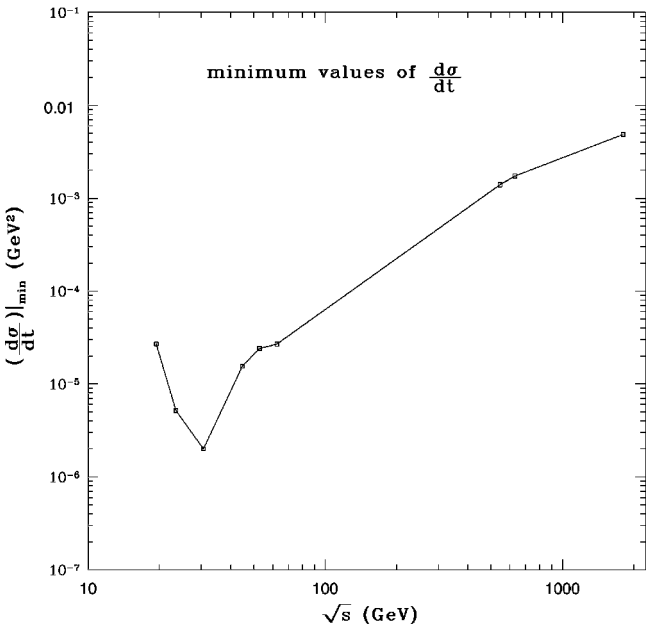

FIG. 3. Energy dependence of the values of the elastic differential cross section at the bottom of the dips.

interval $|t|=1.3-1.5$ GeV^2. This zero is partially filled by the real part of the amplitude which is positive at $|t|=0$ and, according to our parametrization, also decreases nearly exponentially, becoming negative as $|t|$ reaches $0.2-0.3$ GeV^2.

This description is valid for all energies of pp scattering from 19 to 63 GeV. The zeros of the real and imaginary parts of the pp amplitude as a function of the energy are displayed in Fig. 2, where the zeros at 546, 630, and 1800 GeV are also shown. The values of the zeros of Im $T(s,t)$ and of the first zeros of Re $T(s,t)$ decrease monotonically with the energy, while that of the second zero of Re $T(s,t)$ oscillates, being lowest at about 30 GeV. The location of the dips in the differential cross sections are always situated between the zeros of Im $T(s,t)$ and the second zeros of Re $T(s,t)$. The dips are close to the zeros of Im $T(s,t)$, but the shapes in the dip region are strongly influenced by the distance between the zeros of Im $T(s,t)$ and Re $T(s,t)$. At about 30 GeV they are closest, and correspondingly the dips are remarkably pronounced, as shown in Fig. 1.

A similar behavior is also shown by the magnitudes of the differential cross sections at the dip. Figure 3 shows the minimum values of $d\sigma^{el}/dt$ as a function of $\sqrt{s}$, the lowest dip occurring at 30 GeV. The values at 546 and 1800 GeV (which refer to $p\bar{p}$) must be understood only as estimates, while at 630 GeV (also for $p\bar{p}$) the dip is clearly seen in the data.

The sign of the term $\alpha_1'\exp(-\beta_1'|t|)$ in Eq. (2) determines the behavior of $d\sigma^{el}/dt$ in the dip region. The effect of this sign is shown by the dashed lines in Fig. 1, where we disregard the differences in the experimental values of σ^T, B and $\bar{\rho}$ for pp and $p\bar{p}$, keep for both systems the numerical values of all parameters and only invert the sign of α_1'.

As shown in Fig. 11 of our previous work [1], the real part of the amplitude with a positive tail ($\alpha_1'>0$) presents two zeros, the zero near the origin having no influence in the dip region. The second zero, which is close to the zero of the imaginary part is responsible for the pronounced form of the dip. Changing the sign of α_1', the second zero does not exist (or it would be located very far away), so that it is the change of sign in α_1' that causes the flattening of the dips.

We thus see the relation between the behavior of the dips of the elastic differential cross section and the locations of the zeros of the amplitudes in pp and $p\bar{p}$ scattering, and exhibit the role of the sign of the large $|t|$ tail for these systems, in the range $\sqrt{s}=19$–63 GeV. The pp amplitude presents one zero in the imaginary part and two zeros in the real part. The depth of the dips is determined by the proximity between the zeros of the imaginary part and the second zeros of the real part, so that the dips become deeper when these zeros are closer to each other. In $p\bar{p}$ scattering the real amplitude has only the first zero, which occurs far away from the dip region.

The large $|t|$ tail of the differential cross section is described by an exponential term included in the real part of the amplitude. This term, which is the same (except for a sign) for pp and $p\bar{p}$ at all energies from 19 to 63 GeV, is responsible for the change of shape of the dip region when we change from pp to $p\bar{p}$ systems. The sign (which is positive for pp scattering) determines flatter dips in $p\bar{p}$ scattering. The mechanism pointed out by Donnachie and Landshoff [3], is here consistently confirmed by the detailed parametrization, which is remarkably smooth, allowing interpolations for predictions.

[1] F. Pereira and E. Ferreira, Phys. Rev. D **59**, 014008 (1999).

[2] H.G. Dosch, E. Ferreira, and A. Krämer, Phys. Lett. B **289**, 153 (1992); **318**, 197 (1993); Phys. Rev. D **50**, 1992 (1994); E. Ferreira and F. Pereira, *ibid.* **55**, 130 (1997); Phys. Lett. B **399**, 177 (1997).

[3] A. Donnachie and P.V. Landshoff, Phys. Lett. **123B**, 345 (1983); Nucl. Phys. **B231**, 189 (1984).

[4] Data on pp and $\overline{p}p$ systems. (a) A.S. Carrol *et al.*, Phys. Rev. Lett. **33**, 928 (1974); A. Schiz *et al.*, Phys. Rev. D **24**, 26 (1981); L.A. Fajardo *et al.*, *ibid.* **24**, 46 (1981); R.L. Cool *et al.*, *ibid.* **24**, 2821 (1981); R. Rubinstein *et al.*, *ibid.* **30**, 1413 (1984); (b) N. Amos *et al.*, Nucl. Phys. **B262**, 689 (1985); (c) R. Castaldi and G. Sanguinetti, Annu. Rev. Nucl. Part. Sci. **35**, 351 (1985); (d) U. Amaldi and K.R. Schubert, Nucl. Phys. **B166**, 301 (1980); (e) D. Bernard *et al.*, Phys. Lett. B **171**, 142 (1986); C. Augier *et al.*, *ibid.* **316**, 448 (1993); G. Fidecaro *et al.*, *ibid.* **105B**, 309 (1981); (f) N. Amos *et al.*, Phys. Lett. B **243**, 158 (1990); N. Amos *et al.*, *ibid.* **247**, 127 (1990); Phys. Rev. Lett. **68**, 2433 (1992).

[5] E. Nagy *et al.*, Nucl. Phys. **B150**, 221 (1979); K.R. Schubert, *Tables on Nucleon-Nucleon Scattering*, in Landolt-Börnstein *Numerical Data and Functional Relationships in Science and Technology*, New Series, Vol. I/9a (Springer, Berlin, 1979); A. Breakstone *et al.*, Nucl. Phys. **B248**, 253 (1984); Phys. Rev. Lett. **54**, 2180 (1985).

[6] W. Faissler *et al.*, Phys. Rev. D **23**, 33 (1981).

[7] A. Donnachie and P.V. Landshoff, Z. Phys. C **2**, 55 (1979); Phys. Lett. B **387**, 637 (1996).

[8] S. Conetti *et al.*, Phys. Rev. Lett. **41**, 924 (1978).